Available online at www.sciencedirect.com

SciVerse ScienceDirect

Ceramics International 38 (2012) 4173–4180

CERAMICS INTERNATIONAL

www.elsevier.com/locate/ceramint

Preparation of zinc titanate nanoparticles and their photocatalytic behaviors in the photodegradation of humic acid in water

Ya-wen Wang [a], Pei-Hong Yuan [a], Cai-Mei Fan [a,*], Yan Wang [a,b], Guang-Yue Ding [a], Yun-Fang Wang [a]

[a] College of Chemistry and Chemical Engineering, Taiyuan University of Technology, Taiyuan 030024, People's Republic of China
[b] College of Chemistry and bioengineering, Taiyuan University of Science and Technology, Taiyuan 030021, People's Republic of China

Received 1 July 2011; received in revised form 10 January 2012; accepted 28 January 2012
Available online 4 February 2012

Abstract

A series of zinc titanate nanoparticles was successfully synthesized using a simple sol–gel technique. The composites were characterized by thermogravimetric and differential thermal analysis (TG-DTA), X-ray diffraction (XRD) patterns, scanning electron microscope (SEM), X-ray photoelectron spectra (XPS) and UV–vis diffuse reflectance spectra (UV–vis). The photocatalytic activity of samples was investigated by degradation of humic acid (HA) in water under xenon lamp. The sample calcined at 800 °C was found to exhibit much higher photocatalytic activity than the other samples. The investigation of photocatalytic mechanism indicates that the holes (h^+) and $^{\bullet}OH$ radicals may be the major reactive species for the degradation of HA. Meanwhile, the processing parameters such as the light source and the dosage of catalysts play an important role in tuning the photocatalytic activity. The enhancement of photocatalytic activity for the zinc titanate nanoparticles calcined at 800 °C may be attributed to the higher redox ability, coordination of Ti ions and smaller particle size.

Keywords: A. Sol–gel processes; B. Nanocomposites; C. Optical properties; Zinc titanate; Photocatalytic behaviors; Humic acid

1. Introduction

As the main organic components in nature water body, humic acid (HA) has brought a great influence on the health of human beings and the environment. Humic acid is a key component of humic substances which is derived from the decomposition of plants and animals materials. They are a complex mixture of organic compounds. The presence of humic substances can impart an undesirable taste and colour to drinking water. In addition, it has been confirmed that humic substances are the major precursors of disinfectant by-products during chlorination disinfection and trichloromethane class carcinogenic substance [1]. However, humic acid cannot be self-degraded and is difficult to treat by traditional biodegradation method. Therefore, it is imperative to search an effective and practical technique for removing HA from nature water.

Photocatalytic degradation processes have been widely applied as techniques of destruction of organic pollutants in waste water [2–12]. With an appropriate light irradiation, the photocatalyst generates electron/hole pairs with free electrons produced in the empty conduction band and leaving positive holes in the valence band. These electron/hole pairs are capable of initiating a series of chemical reactions that eventually mineralize the pollutants [13].

Recently some researchers were interested in discussing the photophysical, acoustic-optic, and catalytic properties of the ilmenite-type titanates such as $CoTiO_3$, $NiTiO_3$ and $ZnTiO_3$ [14,15]. Dulin and Rase [16] reported that there are three compounds exist in the $ZnO–TiO_2$ system, including Zn_2TiO_4 (cubic), $ZnTiO_3$ (hexagonal) and $Zn_2Ti_3O_8$ (cubic). $ZnTiO_3$ with perovskite structure could be a useful candidate for microwave resonator materials, gas sensors, sorbents for the desulfurization of hot coal gases and paint pigments [17–23]. However, there has not been much work on the photocatalytic activity of zinc titanate particles, which may be used as photocatalyst for the degradation of organic pollutants because its band gap is 3.06 eV. The zinc titanate is usually synthesized

* Corresponding author. Tel.: +86 351 6018193.
E-mail address: fancm@163.com (C.-M. Fan).

0272-8842/$36.00
doi:10.1016/j.ceramint.2012.01.078

via solid-state reaction at high temperatures [24–26], but this method has some drawbacks such as the prepared sample with large particle size and limited chemical homogeneity. In order to improve the properties of zinc titanate particles, some researchers used sol–gel method [27–30] to synthesis zinc titanate nano-crystal powders. In 2009, Kong et al. [31] used a modified alcoholytic method to prepare zinc titanate powder at 800 °C and they also investigated the photocatalytic activity of zinc titanate powders by degradation of the azo dye methyl violet in water under sunlight. So far, to the best of our knowledge, using zinc titanate powders as a photocatalyst in the degradation of HA has not been reported.

In this work, a novel photocatalyst of zinc titanate nanoparticles was first prepared by sol–gel method using citric acid as chelating agent and ethylene glycol as stabilizer. The structure and morphology of the prepared zinc titanate were characterized by various analytical techniques. Then the photocatalytic activity of zinc titanate nanoparticles was investigated by degradation of humic acid in water under xenon lamp. The results indicated that the zinc titanate nanoparticles exhibit good photocatalytic activity on removing humic acid from water. Meanwhile, the possible photodegradation mechanism was also studied by the examination of active species $^{\bullet}OH$, $^{\bullet}O_2^-$ and the holes (h^+) through adding their scavengers.

2. Experimental

2.1. Materials

Ethanol, zinc acetate, tetrabutyl titanate, ethylene glycol, citric acid, isopropanol, sodium bicarbonate and humic acid were purchased from Tianjin Chemical Reagent Factory. Deionized water was used throughout all the experiments. All the chemicals were obtained as analytical grade reagents and used without further purification.

2.2. Synthesis of zinc titanate

Zinc titanate nanoparticles were prepared by the following method. A stoichiometric amount of zinc acetate and tetrabutyl titanate with cationic ratio of Zn: Ti = 1:1 were separately dissolved in water and ethanol (marked as A and B solution separately). Citric acid was then put into the B solution under constant stirring to get a transparency solution (marked as C solution). When the A solution was mixed with the C solution, a small amount of ethylene glycol was added to the solution as a stabilizing agent. The mixed solution was kept stirring at 80 °C for 1 h to form a homogeneous sol. Then the homogeneous sol was aged in an oven in air at 80 °C for 6 h to evaporate excess solvent. Finally, the gel was calcined at 600, 700, 800 and 900 °C in air for 2 h with a heating rate of 5 °C/min, respectively.

2.3. Preparation of humic acid solution

A HA suspension was prepared by adding the HA chemicals into deionized water and gently heating up to 60 °C under magnetic stirring in order to accelerate the dissolution of HA. After the supersaturated HA suspension was cooled down to room temperature, the suspension was filtered by Millipore filter paper. The HA residue on the filter was dried in an oven at 85 °C until the weight stabilized. The HA concentration in the clear solution (filtrate) was calculated by the gravimetric method. The HA solution was stored as a stock solution in a refrigerator at 4 °C for further use.

2.4. Evaluation of photocatalytic activity

Experiment equipment of photocatalytic experiments consists of three parts. The first part is a 500 W xenon lamp in an empty chamber. The second part is a thimble for cooling the xenon lamp by running water. Owing to the continuous cooling, the temperature of the reaction solution is maintained at approximately 32 °C. The third part is a special cylindrical quartz photoreactor with effective reactive volume of 50 mL. The distance between light source and cylindrical quartz photoreactor was about 1.5 cm. The intensity of light was 165,000 lx, measured by a Luxmeter (XYI-III All Digital Luxmeter). At the start of the experiment, the prepared HA solution with initial concentration of 10 mg/L and appropriate amount of photocatalyst were put into the photoreactor. During the photocatalytic reaction, the photocatalytic powder was dispersed by an air bubbler. Portions of approximately 4 mL solutions were taken at selected time intervals and centrifuged at 3000 rpm for 10 min. The concentration of HA in the supernatants was measured with a UV–vis spectrophotometer (Varian Cary 50) at wavelengths of 254 nm. The degradation rate of HA solution was defined according to the equation:

$$D = \left[\frac{A_0 - A_t}{A_0}\right] \times 100\%$$

where A_0 was the absorbance value of initial HA solution, A_t was the absorbance value of degraded HA solution at photocatalytic reaction time "t".

2.5. Characterization

Thermal behavior examination of Zn–Ti-complexed precursor was performed by TG-DTA Analyzer (America PERKEN ELMER 1700) in air to investigate the calcination temperature and possible phase transformation from 20 °C to 1000 °C with a heating rate of 30 °C/min. The resultant phase and crystal structure of the photocatalyst were identified by Rigaku X-ray diffraction (*D*/max-2500) with monochromated Cu Kα radiation at accelerating voltage and applied current are 40 kV and 100 mA, respectively. The data was collected with a scan rate of 8°/min in the range of $2\theta = 20$–$70°$. The microstructure was examined by scanning electron microscopy (SEM, XL30, Philips). The X-ray photoelectron spectroscopy (XPS) measurements were carried out on a spectrometer (XSAM-800, KRATOS Co.) with an Mg Kα anticathode, 12 kV, 11 mA, FRR mode. The UV–vis diffuse reflectance

spectra of the calcined samples were obtained on a Varian Cary 300 UV–vis spectrophotometer.

3. Results and discussion

3.1. TG-DTA analysis

In order to investigate the crystalline behavior and find out the optimum calcining temperature of the citrate complex, thermogravimetric and differential thermal analysis were conducted and the results were illustrated in Fig. 1. Corresponding to the endothermal peaks in DTA curve, the weight loss below 220 °C can be mainly attributed to the evaporation of solvents such as water, alcohol and ethylene glycol. The following weight loss in the temperature range of 220–370 °C can be attributed to the combustion decomposition of organic matter and dehydroxylation of Ti–OH into TiO_2, as corroborated by the exothermic peak at 315 °C in DTA curve. The last weight loss in the temperature 400–600 °C were assigned to the burn out of residual organic components and the crystallization of zinc titanate from an amorphous component, as corroborated by a significant exothermic peak in DTA curve. A broad exothermal peak appeared at around 900 °C in DTA curve, which corresponds to the phase transformation from $ZnTiO_3$ into Zn_2TiO_4.

3.2. XRD analysis

Fig. 2 shows the XRD patterns of the samples calcined at different temperatures. The sample calcined at 600 °C was shown as a mixture of cubic-phase $ZnTiO_3$ (JCPDS Card No. 26-1500), hexagonal-phase $ZnTiO_3$ (JCPDS Card No. 39-0190) and rutile TiO_2 (JCPDS Card No. 21-1276). When the calcined temperature increased (Fig. 2b), the content of cubic-phase $ZnTiO_3$ decreased while hexagonal zinc titanate increased. When the calcined temperature increased to 800 °C, hexagonal-phase $ZnTiO_3$ and cubic-phase $ZnTiO_3$ were the dominant phases. Only trace of the rutile TiO_2 was found [31]. When the calcination temperature increased from 800 to 900 °C, the hexagona-phase $ZnTiO_3$ was not the dominant phase. The peaks related to cubic-phase Zn_2TiO_4 (JCPDS Card No. 25-1164) and rutile TiO_2 appeared, which might be attributed to the decomposition of hexagonal-phase $ZnTiO_3$ into cubic spine (Zn_2TiO_4) and rutile (TiO_2) at much higher temperature [30].

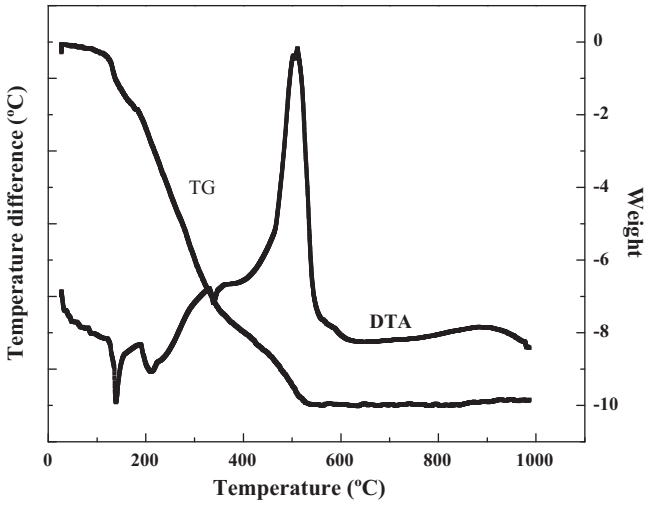

Fig. 1. The TG and DTA curves of zinc titanate precursor powder.

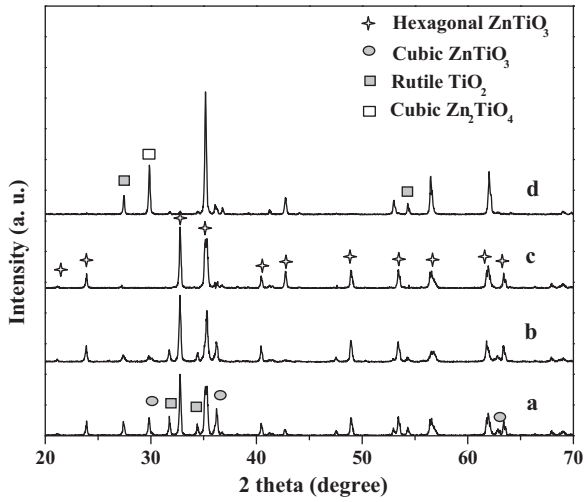

Fig. 2. XRD patterns of the samples calcined at different temperatures (a) 600 °C, (b) 700 °C (c) 800 °C and (d) 900 °C.

3.3. SEM analysis

Fig. 3 gives the SEM micrographs of the samples calcined at various temperatures: (a) 700 °C, (b) 800 °C and (c) 900 °C. The particles calcined at 700 °C and 900 °C were about 120–220 nm and 230–300 nm, respectively. However, the particles calcined at 800 °C were about 80–150 nm, which is much smaller than the particles in samples calcined at 700 °C and 900 °C.

3.4. XPS analysis

X-ray photoelectron spectroscopy (XPS) can provide chemical information such as the oxidation state, as well as the semiquantitative composition of the surface, and is a very useful method for studying surface properties. Fig. 4(a) displays the XPS results for the samples calcined at 800 °C. The elements Zn, Ti and O were detected. Fig. 4(b) suggested that the binding energie for $2p_{3/2}$ of Zn was 1020.4 eV, which is in agreement with that reported in the literature [31] for ZnO lattice. It can be concluded that Zn was existed in $ZnTiO_3$ sample in Zn^{2+} states.

Fig. 4(c) suggested that the binding energies for $Ti2p_{3/2}$ can be fitted into two peaks at 457.7 eV and 458.9 eV. This implied that there were two different chemical environments of Ti ions existed in the sample. The first Ti ions could be assigned to an octahedral environment, and the second Ti ions were in a tetrahedral environment [32–34]. It is known that Ti ions on the external surface of TiO_2 are partly four- or five-coordinated, especially in particles with size smaller than 20 nm [35]. These unsaturated-coordinated species may exhibit different reactivities and surface

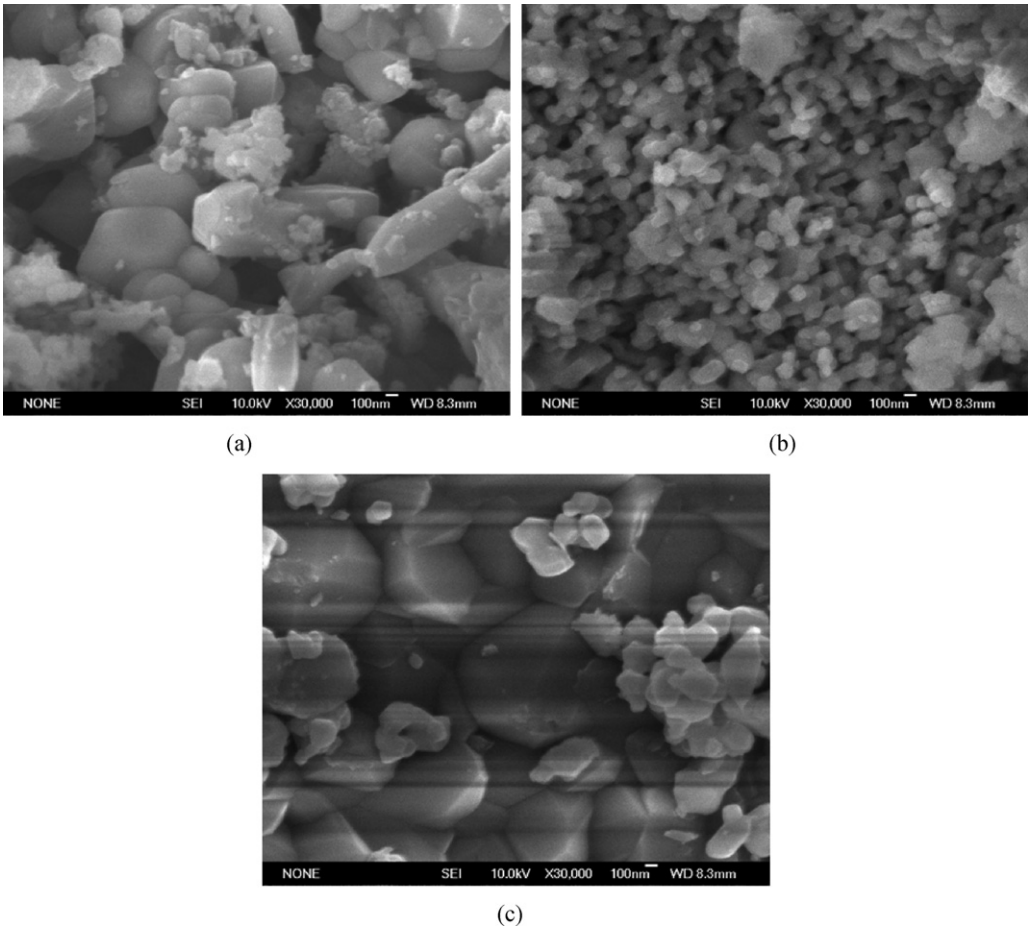

Fig. 3. SEM images of zinc titanate calcined at (a) 700 °C, (b) 800 °C and (c) 900 °C.

properties [36]. Therefore, photocatalytic activity of the zinc titanate calcined at 800 °C is worth exploring.

Fig. 4(d) showed that the O1s region was decomposed into three contributions. The dominant contribution was attributed to O–Ti bonds (529.6 eV). The other two kinds of oxygen contributions could be counted by the O–Zn bonds (530.1 eV) [37] and the hydroxyl groups (531.9 eV), respectively.

3.5. UV–vis diffuses reflectance spectra and band gap

Fig. 5 displayed the UV–vis diffuse reflectance spectra (UV–vis DRS) of the samples calcined at 600, 700, 800 and 900 °C (Fig. 5a). It can be seen the optical absorption of all the photocatalysts started at about 425 nm (red shift). The band gap were determined by the following equation using the date of optical absorption vs. wavelength near the band edge [31],

$(\alpha h\upsilon)^{1/2} = A(h\upsilon - E_g)$where α, υ, A and E_g are absorption coefficient, light frequency, proportionality constant, and band gap, respectively. The band gap energy of zinc titanate can be estimated by the intercept of the tangent to the x-axis from plots of $(\alpha h\upsilon)^{1/2}$ vs. photon energy ($h\upsilon$). As shown in Fig. 5b, the band gaps optically obtained in such a way were approximately 2.73, 2.7, 2.85 and 2.79 eV for the samples calcined at 600, 700, 800, and 900 °C, respectively. This suggests that the zinc titanate has a potential property for photocatalytic decomposition of organic contaminants under sunlight irradiation.

3.6. Photocatalytic activities of the zinc titanate calcined at different temperature

The photocatalytic activity test were all conducted under the amount of photocatalyst of 0.8 g/L. Fig. 6 showed the degradation of humic acid solution using different samples calcinated at 600, 700, 800 and 900 °C under xenon lamp irradiation for 2.5 h. The results indicated that the photocatalytic activities of samples were increased with the increasing of the calcined temperature when the calcined temperature is below 800 °C. The sample calcined at 800 °C was found to be the best photocatalyst for the removal of HA. When the calcined temperature increased to 900 °C, the photocatalytic activity of samples was decreased. This feature indicated that the calcined temperature has an important influence on the photoactivity of the samples.

3.7. Investigation on active species

The photocatalytic activity is governed by various factors such as surface area, the band gap, the oxidation potential of photogenerated holes, and the separation efficiency of

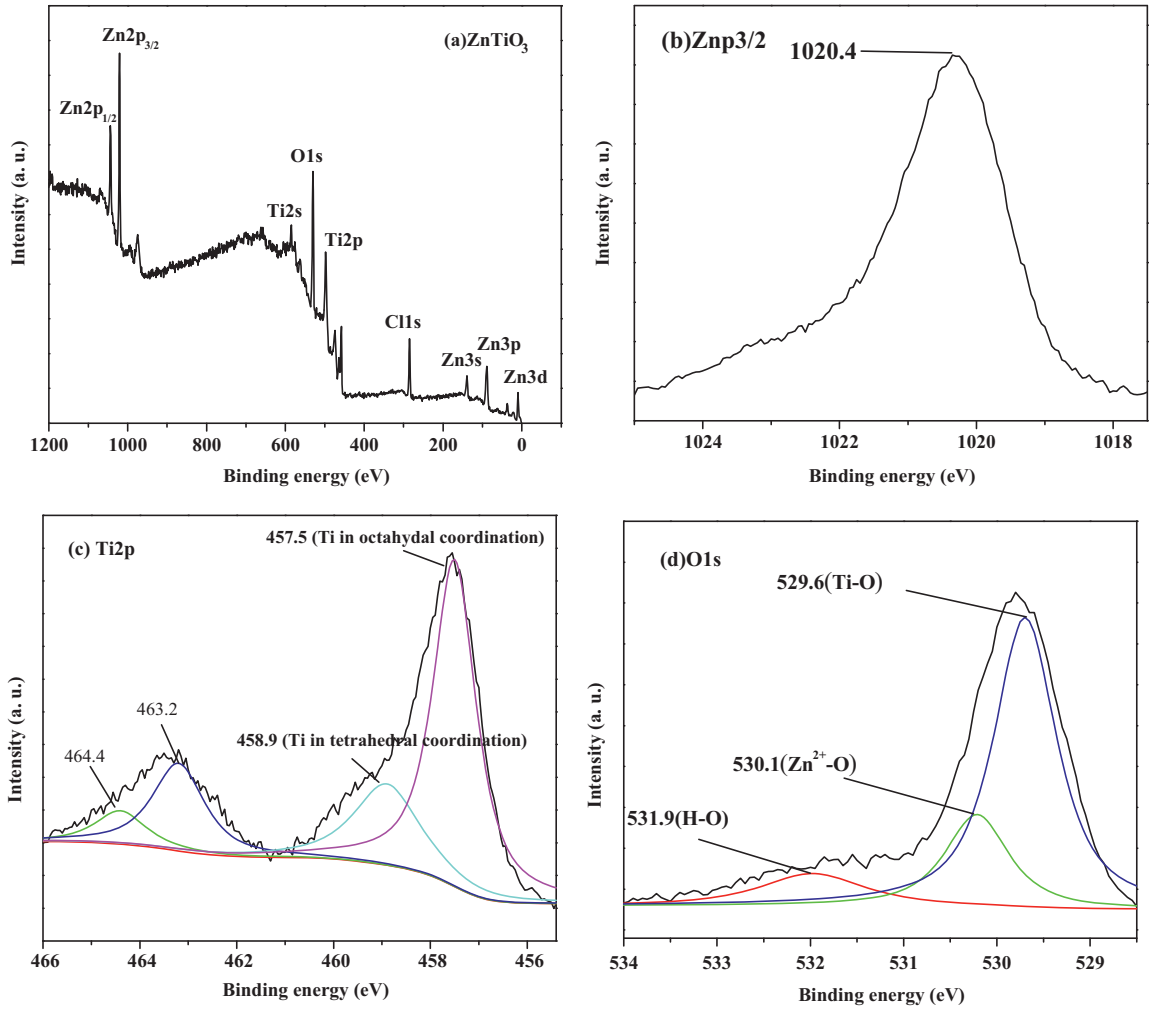

Fig. 4. Survey XPS (a) and high-resolution spectra of Zn2p (b), Ti2p (c) and O1s (d) of the sample calcined at 800 °C.

photogenerated electrons and holes (h^+) [38]. In general, during the photocatalytic degradation process for photocatalysts, the irradiation induces the formation of electrons (e^-) and holes (h^+) on the photocatalysts surface. The photogenerated holes (h^+) react with the adsorbed OH^- and high activity $^{\bullet}OH$ radicals are produced. The $^{\bullet}OH$ radicals can react with any substances non-selectively. The photogenerated holes (h^+) can also deprive the electrons of organic pollutant directly and oxidize it into radicals. Meanwhile, dissolved oxygen (DO) in water can capture electron and produce O_2^- which react with

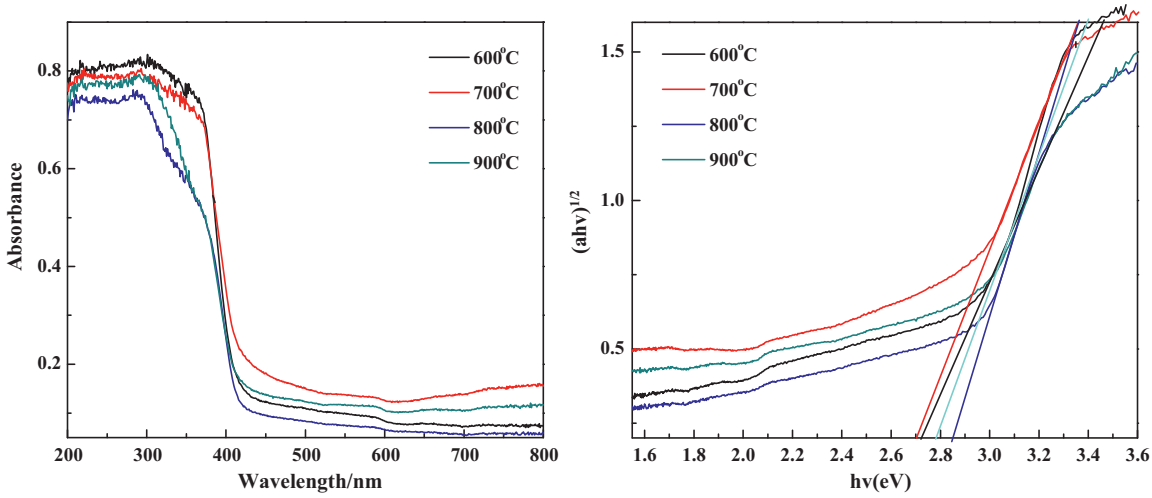

Fig. 5. UV–vis diffuse reflectance spectra (a) and plots of the $(\alpha h\upsilon)^{1/2}$ vs. the energy of absorbed light of the samples calcined at 600 °C, 700 °C, 800 °C, 900 °C.

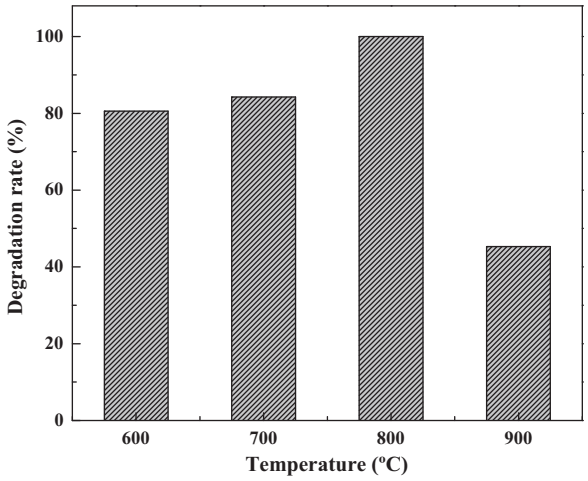

Fig. 6. The effect of degradation of HA solution of the samples calcined at different temperatures after irradiation 2.5 h.

humic acid or humic acid intermediates. Moreover, DO can further form into $^{\bullet}OH$ under protonation resulting [39] in degradation of humic acid.

In the photocatalytic degradation process of HA, the holes (h^+), $^{\bullet}O_2^-$ and $^{\bullet}OH$ are considered to be the reactive species [40]. To ascertain the role of the major reactive species in the degradation process of HA, a series of tests were conducted by added some sacrificial agents, such as isopropanol (i-PrOH) ($c = 0.01$ mol L^{-1}), $NaHCO_3$ ($c = 0.01$ mol L^{-1}) [41] and N_2 (replace O_2) into reaction solution to confirm the specific reactive species. The results were showed in Fig. 7. It can be seen that when no scavenger added to the reaction solution, 100% HA was degraded. When $^{\bullet}O^{2-}$ scavenger, N_2, was introduced from the bottom of the photoreactor, about 87% HA was degraded, showing that the $^{\bullet}O^{2-}$ has minor influence on the activity of HA degradation in this process. However, when the holes (h^+) and $^{\bullet}OH$ scavenger, $NaHCO_3$, was put into the photocatalytic reaction systems, only about 32% HA was degraded. This indicated that holes (h^+) and/or

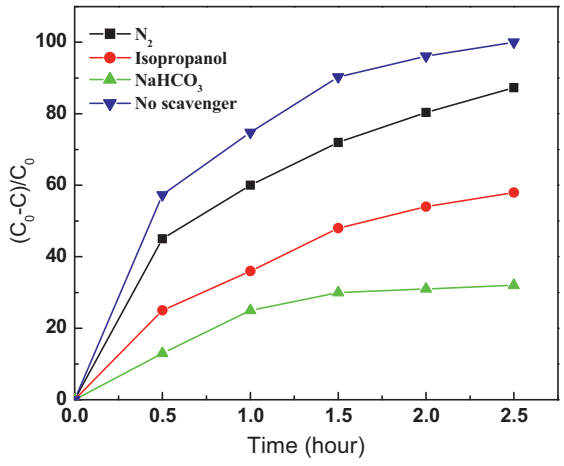

Fig. 7. Effect of the scavengers on the degradation rate of the sample calcined at 800 °C.

$^{\bullet}OH$ played an important role in the photocatalytic process. When $^{\bullet}OH$ scavenger, i-PrOH, was put into the degradation systems, about 58% HA was degraded. It is suggested that $^{\bullet}OH$ radicals really played a major role in the photodegradation of HA. These results indicated that both photogenerated holes (h^+) and $^{\bullet}OH$ played an important role in the photodegradation of HA.

The high photocatalytic activity of the sample calcined at 800 °C can be explained as follows. First, it is commonly accepted that a larger band gap corresponds to more powerful redox ability [41]. Since the sample calcined at 800 °C has a larger band gap than the samples calcined at other temperatures, its oxidizing ability should be stronger. Yamashita et al. [42] reported that tetrahedral titanium oxide moieties on the surface layer of the silica glass could be responsible for the high photocatalytic activity. Second, we believe that the Ti ions in tetrahedral coordination offer a number of benefits. These tetrahedrally coordinated Ti ions can adsorb water and oxygen in air to produce more hydroxyl groups on the surface of zinc titanate. Moreover, the adsorbed water and oxygen by the Ti ions in tetrahedral coordination can stabilize the photoexcited hole and electron pairs [43]. This would slow the rate of e^-–h^+ recombination and increase the photocatalytic activity. Third, particle size is an important parameter for catalysis in general since it directly affects the specific surface area of a catalyst. With a smaller particle size, the number of active surface sites increases, as so does the surface charge carrier transfer rate in photocatalysis [44]. In our experiments, the sample calcined at 800 °C have the smaller particle size than the samples calcined at other temperatures, which could increase the number of active surface sites, the surface charge carrier transfer rate and the adsorption of reactant molecules. Therefore, it is reasonable to find that the sample calcined at 800 °C showed enhanced photocatalytic activity than the others.

3.8. Effect of the amount of photocatalyst on the degradation rate

For economic removal of humic acid from nature water, it is necessary to find the optimum amount of catalyst for photocatalytic degradation. Fig. 8 showed that the degradation rate increased with the increasing amount of photocatalyst. However, when the amount of photocatalyst exceeded 0.8 g/L, the photocatalytic activity decreased. It is well known that when the amount of photoctalyst is less, the less photo energy be changed into chemical energy. Therefore, the photocatalytic activity of the photocatalyst increased with the addition of photocatalyst. However, when the amount of the photocatalyst is excessive, the action of light scattering is aggravated by excessive catalyst suspended in aqueous solution. The catalyst particles screen mutually, which would reduce the surface area of the catalyst and lead to the decreased of photocatalytic activity [45]. Therefore, an appropriate amount of photocatalyst is an important factor for the photocatalytic reaction. In order to achieve the best decomposition effect, 0.8 g/L of photocatalyst was chosen in the following experiments.

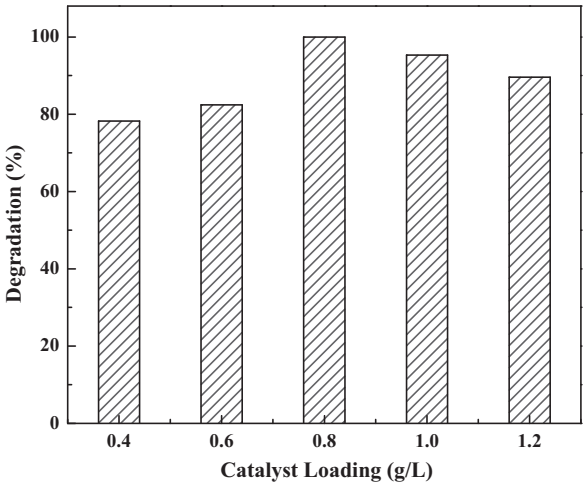

Fig. 8. Effect on the degradation rate for the sample calcined at 800 °C of different amount.

3.9. Comparison of photolysis, photocatalysis and adsorption of HA

It is well known that the first step of organic oxidative decomposition is oxidation reaction of the organic molecules with hydroxyl radicals produced on the photocatalyst surface. Adsorption process of organic pollutant on photocatalyst is very important for the heterogeneous photocatalytic reactions [46]. In order to understand the photocatalytic performance better, Fig. 9 showed the comparative results of the changes of degradation rate with reactive time in adsorption, photolysis and photocatalysis process, respectively. The photocatalysis of P25 was added for comparing. The results showed that 25% and 14.7% of HA were removed for adsorption and photolysis respectively after 2.5 h, while the degradation rate of photocatalytic process for sample calcined at 800 °C reached 100%, which has similar photocatalytic ability to P25. For the sample calcined at 800 °C, at beginning of the photocatalytic test, the process is composed of photolysis, photocatalysis and adsorption at the same time, which would lead to the rate of photocatalytic reaction at this period much higher than the rates at other period. After that, both adsorption and photolysis achieved equilibrium and had no positive influence on the photocatalytic rate, the whole photoreaction rate is decrease.

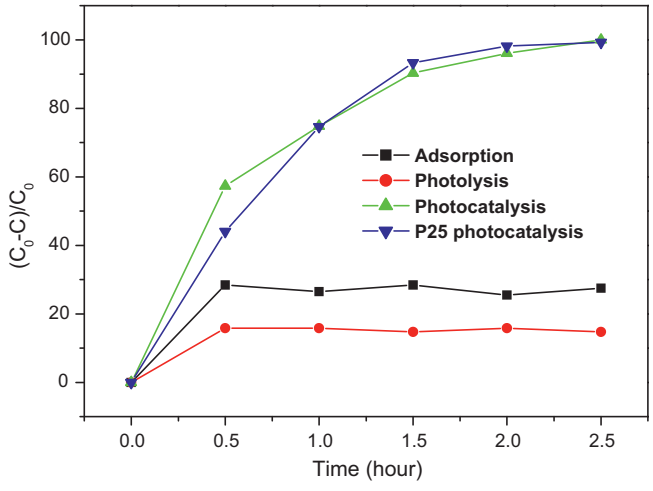

Fig. 9. Comparison of photolysis, photocatalysis and adsorption of HA for sample calcined at 800 °C and the photocatalysis of HA for P25 under illumination of xenon light for 2.5 h.

4. Conclusions

In this study, the zinc titanate nanoparticles have been prepared through sol–gel method using citric acid as chelating agent and ethylene glycol as stabilizer. The structure, morphology and photocatalytic activity of obtained samples were characterized by various analytical techniques. The photocatalytic activity of zinc titanate was evaluated by degrading the humic acid solution under the irradiation of sunlight and xenon lamp. The amount of photocatalyst, calcined temperature of zinc titanate and light source all has a great effect on the degradation rate of humic acid. The optimal amount of catalyst and the favourite calcined temperature of zinc titanate are 0.8 g/L and 800 °C, respectively. The holes (h^+) and $^{\bullet}OH$ radicals are the major reactive species for the photocatalytic reactions. The enhancement of photocatalytic activity for the zinc titanate calcined at 800 °C may be attributed to the higher redox ability, coordination of Ti ions and smaller particle size.

Acknowledgments

This work was financially supported by the National Natural Science Foundation of China (No. 20876104) and the Science and Technology Foundation of Shanxi Province, China (No. 20090311082).

References

[1] X.Z. Li, C.M. Fan, Y.P. Su, Enhancement of photocatalytic oxidation of humic acid in TiO_2 suspensions by increasing cation strength, Chemosphere 48 (2002) 453–460.
[2] S.C. Pillai, P. Periyat, R. George, D.E. McCormack, M.K. Seery, H. Hayden, J. Colreavy, D. Corr, S.J. Hinder, Synthesis of high-temperature stable anatase TiO_2 photocatalyst, J. Phys. Chem. C 111 (2007) 1605–1611.
[3] A. Muruganandham, N. Shobana, A. Swaminathan, Optimization of solar photocatalytic degradation conditions of reactive yellow14 azo dye in aqueous TiO_2, J. Mol. Catal. A: Chem. 246 (2006) 154–161.
[4] W.S. Kuo, P.H. Ho, Solar photocatalytic decolorization of dyes in solution with TiO_2 film, Dyes Pigments 71 (2006) 212–217.
[5] S. Sakthivel, B. Neppolian, M.V. Shankar, B. Arabindoo, M. Palanichamy, V. Murugesan, Solar photocatalytic degradation of azo dye: comparison of photocatalytic efficiency of ZnO and TiO_2, Sol. Energy Mater. Sol. Cells 80 (2003) 65–82.
[6] S.K. Kansal, M. Singh, D. Sud, Studies on photodegradation of two commercial dyes in aqueous phase using different photocatalysts, J. Hazard. Mater. 141 (2007) 581–590.
[7] E. Evgenidou, K. Fytianos, I. Poulios, Semiconductor-sensitized photodegradation of dichlorvos in water using TiO_2 and ZnO as catalysts, Appl. Catal. B: Environ. 59 (2005) 81–89.
[8] M. Muruganandham, N. Sobana, M. Swaminathan, Solar assisted photocatalytic and photochemical degradation of reactive black 5, J. Hazard. Mater. 137 (2006) 1371–1376.

[9] B. Neppolian, H.C. Choi, S. Sakthivel, B. Arabindoo, V. Murugesan, Solar/UV induced photocatalytic degradation of three commercial textile dyes, J. Hazard. Mater. 89 (2002) 303–317.
[10] S.K. Pardeshi, A.B. Patil, Solar photocatalytic degradation of resorcinol a model endocrine disrupter in water using zinc oxide, J. Hazard. Mater. 163 (2009) 403–409.
[11] C. Karunakaran, S. Senthilvelan, S. Karuthapandian, Solar photooxidation of aniline on ZnO surfaces, Sol. Energy Mater. Sol. Cells 89 (2005) 391–402.
[12] K.M. Parida, S. Parija, Photocatalytic degradation of phenol under solar radiation using microwave irradiated zinc oxide, Sol. Energy 80 (2006) 1048–1054.
[13] J. Nishio, M. Tokumura, H.T. Znad, Y. Kawase, Photocatalytic decolorization of azo-dye with zinc oxide powder in an external UV light irradiation slurry photoreactor, J. Hazard. Mater. B 138 (2006) 106–115.
[14] L. Zhou, S.Y. Zhang, J.C. Cheng, L.D. Zhang, Z.H. Zeng, Optical absorptions of nanoscaled $CoTiO_3$ and $NiTiO_3$, Mater. Sci. Eng. B 49 (1997) 117–122.
[15] S.F. Wang, F. Gu, C.F. Song, D. Xu, D.R. Yuan, G.J. Zhou, Y.X. Qi, Photoluminescence characteristicsof Pb^{2+} ion in sol–gel derived $ZnTiO_3$ nanocrystals, Inorg. Chem. Commun. 6 (2003) 185–188.
[16] F.H. Dulin, D.E. Rnse, Phase Equilibria in the System ZnO–TiO_2, J. Am. Ceram. Soc. 43 (1960) 125–131.
[17] H.T. Kim, J.D. Byun, Y. Kim, Microstructure and microwave dielectric properties of modified zinc titanates (II), Mater. Res. Bull. 33 (1998) 975–986.
[18] Z.X. Chen, J. Van der Berg, W. Koot, R. Van der Berg, J. Van Mechelen, A. Derking, Preparation of zinc titanate thin films by low-pressure metalorganic chemical vapor deposition, J. Am. Ceram. Soc. 78 (1995) 2993–3001.
[19] H. Obayashi, Y. Sakurai, T. Gejo, Perovskite-type oxides as ethanol sensors, J.Solid State Chem. 17 (1976) 299–303.
[20] Z.X. Chen, A. Derking, W. Koot, M.P. van Dijk, Dehydrogenation of isobutane over zinc titanate thin film catalysts, J. Catal. 161 (1996) 730–741.
[21] S.F. Wang, F. Gu, M.K. Lü, C.F. Song, D. Xu, D.R. Yuan, S.W. Liu, Photoluminescence of sol–gel derived $ZnTiO_3$: Ni^{2+} nanocrystals, Chem. Phys. Lett. 373 (2003) 223–227.
[22] S.F. Wang, M.K. Lü, F. Gu, C.F. Song, D. Xu, D.R. Yuan, G.J. Zhou, Y.X. Qi, Photoluminescence characteristics of Pb^{2+} ion in sol–gel derived $ZnTiO_3$ nanocrystals, Inorg. Chem. Commun. 6 (2003) 185–188.
[23] W. Wu, Y.W. Cai, J.F. Chen, S.L. Shen, A. Martin, L.X. Wen, Preparation and properties of composite particles made by nano zinc oxide coated with titanium dioxide, J. Mater. Sci. 41 (2006) 5845–5850.
[24] F.H. Dulin, D.E. Rase, Phase equilibria in the system ZnO–TiO_2, J. Am. Ceram. Soc. 43 (1960) 125–131.
[25] X.H. Zeng, Y.Y. Liu, X.Y. Wang, W.C. Yin, L. Wang, H.X. Guo, Preparation of nanocrystalline $PbTiO_3$ by accelerated sol–gel process, Mater. Chem. Phys. 77 (2002) 209–214.
[26] Z. Surowiak, M.F. Kupriyanov, D. Czekaj, Properties of nanocrystalline ferroelectric PZT ceramics, J. Eur. Ceram. Soc. 21 (2001) 1377–1381.
[27] Y.S. Chang, Y.H. Chang, I.J. Chen, Synthesis and characterization of zinc titanate nano-crystal powders by sol–gel technique, J. Cryst. Growth 243 (2002) 319–326.
[28] S.F. Wang, F. Gu, C.F. Song, S.W. Liu, D.R. Yuan, Preparation and characterization of sol–gel derived $ZnTiO_3$ nanocrystals, Mater. Res. Bull. 38 (2003) 1283–1288.
[29] L. Hou, Y.D. Hou, M.K. Zhu, J.L. Tang, J.B. Liu, H. Wang, H. Yan, Formation and transformation of $ZnTiO_3$ prepared by sol–gel process, Mater. Lett. 59 (2005) 197–200.
[30] M.R. Mohammadi, D.J. Fray, Low temperature nanostructured zinc titanate by an aqueous particulate sol–gel route: optimisation of heat treatment condition based on Zn: Ti molar ratio, Eur. Ceram. Soc. 30 (2010) 947–961.
[31] J.Z. Kong, A.D. Li, H.F. Zhai, H. Li, Q.Y. Yan, J. Ma, D. Wu, Preparation, characterization and photocatalytic properties of $ZnTiO_3$ powders, J. Hazard. Mater. 171 (2009) 918–923.
[32] F.B. Li, X.Y. Li, Photocatalytic properties of gold/gold ion-modified titanium dioxide for wastewater treatment, Appl. Catal. A: Gen. 228 (2002) 15–27.
[33] Y. Hu, O.K. Tan, J.S. Pan, X. Yao, A new form of nanosized $SrTiO_3$ material for near-human-body temperature oxygen sensing applications, J. Phys. Chem. B 108 (2004) 11214–11218.
[34] J.C. Yu, L.Z.H. Zhang, Z.H. Zheng, J.C. Zhao, Synthesis and characterization of phosphated mesoporous titanium dioxide with high photocatalytic activity, Chem. Mater. 15 (2003) 2280–2286.
[35] Y. Suda, T. Morimoto, Molecularly adsorbed water on the bare surface of titania (rutile), Langmuir 3 (1987) 786–788.
[36] T. Rajh, J.M. Nedeljkovic, L.X. Chen, O. Poluektov, M.C. Thurnauer, Improving optical and charge separation properties of nanocrystalline TiO_2 by surface modification with vitamin C, J. Phys. Chem. B 103 (1999) 3515–3519.
[37] Z.I. Bingtao, B.A. Qixian, C.U.I. Jianzhong, X.U. Guangming, Study on axial changes of As-cast structures of Al-alloy sample treated by the novel SPMF technique, Scr. Mater. 43 (2000) 377–380.
[38] M.R. Hoffmann, S.T. Martin, W. Choi, D.W. Bahnemann, Environmental applications of semiconductor photocatalysis, Chem. Rev. 95 (1995) 69–96.
[39] C.M. Fan, Y.Q. M, X.G. Hao, Y.P. Sun, X.J. Li, F.B. Li, Adsorption and photocatalytic degradation of phenol over TiO_2/ACF, Trans. Nonferrous Met. Soc. China 13 (2003) 452–456.
[40] Y.X. Chen, S.Y. Yang, K. Wang, L.P. Lou, Role of primary active species and TiO_2 surface characteristic in UV-illuminated photodegradation of acid orange 7, J. Photochem. Photobiol. A 172 (2005) 47–54.
[41] J. Lin, J.C. Yu, D. Lo, S.K. Lam, Photocatalytic activity of rutile $Ti_{1-x}Sn_xO_2$ solid solutions, J. Catal. 183 (1999) 368–372.
[42] H. Yamashita, M. Honda, M. Harada, Y. Ichihashi, M. Anpo, T. Hirao, N. Itoh, N. Iwamoto, Preparation of titanium oxide photocatalysts anchored on porous silica glass by a metal ion-implantation method and their photocatalytic reactivities for the degradation of 2-propanol diluted in water, J. Phys. Chem. B 102 (1998) 10707–10711.
[43] S.J. Tsai, S. Cheng, Effect of TiO_2 crystalline structure in photocatalytic degradation of phenolic contaminants, Catal. Today 33 (1997) 227–237.
[44] Z. Zhang, C.C. Wang, R. Zakaria, Y. Ying, Role of particle size in nanocrystalline TiO_2-based photocatalysts, J. Phys. Chem. B 102 (1998) 10871–10878.
[45] Y.M. Cui, W.Z.H. Zhang, Degradation of BPB in photocatalysis enhanced by photosensitizer, Sun. Rare Metals 25 (2006) 138–143.
[46] H. Liu, S.A. Cheng, J.Q. Zhang, Titanium dioxide as photocatalyst on porous nickel: adsorption and the photocatalytic degradation of sulfosalicylic acid, Chemosphere 38 (1999) 283–292.